

ORIGINAL RESEARCH

Low-molecular-weight hyaluronan (LMW-HA) accelerates lymph node metastasis of melanoma cells by inducing disruption of lymphatic intercellular adhesion

Yan Du^{a,b,*}, Manlin Cao^{c,*}, Yiwen Liu^a, Yiqing He^a, Cuixia Yang^a, Man Wu^a, Guoliang Zhang^a, and Feng Gao^{a,b}

^aDepartment of Molecular Biology, Shanghai Jiao Tong University Affiliated Sixth People's Hospital, Shanghai, P.R. China; ^bDepartment of Clinical Laboratory, Shanghai Sixth People's Hospital, Shanghai Jiao Tong University School of Medicine, Shanghai, P.R. China; ^cDepartment of Rehabilitation Medicine, Shanghai Sixth People's Hospital, Shanghai Jiao Tong University School of Medicine, Shanghai, P.R. China

ABSTRACT

Endothelial integrity defects initiate lymphatic metastasis of tumor cells. Low-molecular-weight hyaluronan (LMW-HA) derived from plasma and interstitial fluid was reported to be associated with tumor lymphatic metastasis. In addition, LMW-HA was proved to disrupt lymphatic vessel endothelium integrity, thus promoting lymphatic metastasis of tumor cells. Until now, there are few reports on how LMW-HA modulates lymphatic endothelial cells adhesion junctions and affects cancer cells metastasizing into lymph vessels. The aim of our study is to unravel the novel mechanism of LMW-HA in mediating tumor lymphatic metastasis. Here, we employed a melanoma metastasis model to investigate whether LMW-HA facilitates tumor cells transferring from foci to remote lymph nodes by disrupting the lymphatic endothelial integrity. Our data indicate that LMW-HA significantly induces metastasis of melanoma cells to lymph nodes and accelerates interstitial-lymphatic flow *in vivo*. Further experiments show that increased migration of melanoma cells across human dermal lymphatic endothelial cell (HDLEC) monolayers is accompanied by impaired lymphatic endothelial barrier function and increased permeability. The mechanism study reveals that VE-cadherin- β -catenin pathway and relevant signals are involved in modulating the interactions between endothelial cells and that a significant inhibition of lymphatic endothelium disruption is observed when antibodies to the LMW-HA receptor (LYVE-1) are present. Thus, our findings demonstrate a disruptive effect of LMW-HA on lymphatic endothelium continuity which leads to a promotion on melanoma lymphatic metastasis and also suggest a cellular signaling mechanism associated with VE-cadherin-mediated lymphatic intercellular junctions.

ARTICLE HISTORY

Received 27 June 2016
Revised 29 August 2016
Accepted 31 August 2016

KEYWORDS

HDLEC; LMW-HA; lymphatic intercellular adhesion; lymphatic metastasis; melanoma

Introduction

Lymphatic metastasis is the primary cause of morbidity and mortality in many solid tumors, such as head and neck squamous cell carcinoma, breast cancer, stomach cancer, and melanoma. In malignant melanoma, approximately 60% of metastasis occurs in regional lymph nodes (LNs), and regional LN metastasis is the most powerful predictor of prognosis.¹ To date, the exact mechanism underlying lymphatic metastasis is poorly understood.


Recently, abundant evidence has indicated that tumor cell metastasis to LNs is governed by complex factors in which the importance of tumor microenvironment appears to be a focus.² Many studies are now being devoted to determine how extracellular matrix (ECM) components in specific tumor microenvironment initiate and facilitate cancer development.³ A recent study highlighted the importance of non-cellular components surrounding tumors, noting that ECM components can drive cancer malignancy by directly promoting cellular transformation and metastasis.⁴ Hyaluronan (HA), the most abundant ECM component that facilitates tissue homeostasis, is an unbranched polymer composed of repeating glucuronic acid and N-acetyl glucosamine disaccharide units in physiological

conditions with a high molecular weight ($\sim 10^7$ Da). Following tissue injury or tumorigenesis, elevations in hyaluronidase activity and generation of reactive oxygen species cause excess accumulation of low-molecular-weight hyaluronan (LMW-HA), which is derived from high-molecular-weight hyaluronan (HMW-HA) degradation.⁵ Differences in HA chain length can provoke distinct biological functions.^{6,7}

High concentrations of LMW-HA have been detected in the urine of high-grade bladder cancer patients,⁸ and in the saliva of high-stage head and neck squamous cell carcinoma patients.⁹ More importantly, one study investigated the levels of hyaluronan fragments ranging from 6–25 disaccharides in the interstitial fluid of colorectal tumors, and found that elevated LMW-HA levels were associated with lymphatic vessel invasion by tumor cells and LN metastasis.¹⁰ Similarly, our previous work showed that serum levels of LMW-HA, but not total HA, clearly correlated with LN metastasis in breast cancer.¹¹ Besides of these findings, LMW-HA has also been reported to induce lymphangiogenesis,¹² which is similar to the angiogenesis promoted by LMW-HA or hyaluronan fragments. As tumor cell metastasis via lymphatic vessels is a complicated process

CONTACT Feng Gao  gao3507@126.com  Shanghai Jiao Tong University Affiliated Sixth People's Hospital, 600 Yishan Road, Shanghai, P.R. China.

*These authors contributed equally to this work.

 Supplemental data for this article can be accessed on the publisher's website.

© 2016 Taylor & Francis Group, LLC

requiring new lymphatic vessel formation or lymphangiogenesis, as well as lymphatic vessel infiltration by tumor cells,^{13,14} it is necessary to elucidate the other mechanisms by which this process occurs, in addition to lymphangiogenesis. It is accepted that endothelial cell disconnection or endothelial barrier breakdown is essential for cancer cell leakage into vessels.¹⁵ A number of growth factors are known to influence endothelial cell integrity, including vascular endothelial growth factor (VEGF) and angiopoietin/TIE family members.^{16,17} For example, down-regulation of barrier function of lymphatic endothelial monolayer has been shown to facilitate sarcoma cell entry into the lymphatic circulation by VEGF-D.¹⁸ However, these data are not sufficient to explain the mechanisms by which cancer cells disseminate into vessels surrounding tumors. In addition to growth factors, ECM components and their degradative products are other kinds of active stimulating factors during remodeling of tumor microenvironment. For example, degradation of high-molecular-weight hyaluronan results in accumulation of excess amounts of LMW-HA, which is proangiogenic.¹⁹ Studies have indicated that impairment of blood vascular barrier could be mediated by LMW-HA and an accelerating vascular metastasis of cancer cells was followed.^{20,21} To date, there are no reports regarding how LMW-HA modulates lymphatic endothelial cell junctions or facilitates cancer cell metastasis through lymph vessels. As lymphatic vascular endothelial cells are similar to blood vessels in terms of their proliferation behavior and HA receptor expression patterns, it is reasonable to assume that LMW-HA regulates lymphatic endothelial intercellular adhesion by binding to lymphatic endothelial hyaluronan receptor-1 (LYVE-1) and thus accelerates tumor cell migration into the lumen of lymphatic vessels.

In this study, we employed a mouse model in which melanoma cells were transferred from the interstitial fluid into the lymphatic lumen to elucidate the role of LMW-HA in modulating tumor cell metastasis via lymphatic vessels. We found that *in vivo* LMW-HA administration promoted local melanoma cell metastasis from the footpad to the popliteal LNs. We also demonstrated that LMW-HA disrupted the lymphatic endothelial barrier and increased B16F10 melanoma cell migration across the lymphatic endothelium. A subsequent mechanism investigation indicated that vascular endothelial (VE)-cadherin and several related signaling molecules were associated with LMW-HA-induced disruption of endothelial barrier integrity.

Our study suggests that accumulation of excess hyaluronan fragments in the tumor microenvironment is of great importance in tumor lymphatic metastasis and may provide new insights regarding possible therapies for tumor lymphatic metastasis in the future.

Results

LMW-HA enhances lymph node metastasis of melanoma cells by inducing disruption of lymphatic intercellular adhesion in mice

To assess the effects of LMW-HA on LN metastasis *in vivo*, we used a mouse model and inoculated B16F10 melanoma cells into the hind footpads of syngeneic mice to determine if local abnormal accumulation of LMW-HA around tumor

mimicking tumor microenvironment could disrupt lymphatic endothelial integrity and thus lead to tumor cell leakage into lymphatic vessels. The primary tumors in the footpads became grossly visible after 7 d, and macroscopic metastases were observed in the LNs of some mice. The popliteal LNs were collected to evaluate these early metastases by quantifying the mRNA levels of TRP, a melanocyte-specific marker. qRT-PCR results indicated that TRP mRNA levels were significantly increased by as much as 32-fold in LMW-HA-treated mice compared with control mice (Fig. 1A; $p < 0.05$). However, the levels noted in HMW-HA-treated mice were similar to those noted in control mice (Fig. 1A). On day 17 after the first injection, the primary tumors in the footpads were approximately 1 cm in diameter. To evaluate tumor metastasis at a later stage, we dissected the popliteal LNs to identify metastatic foci. All the nodes from LMW-HA-treated mice contained totally black metastatic foci ranging from 2–7 mm in size, whereas only some of the LNs from HMW-HA- or medium-treated mice exhibited smaller macroscopic metastatic foci (Fig. 1B). Our results indicate that LMW-HA promotes tumor cell metastasis via draining LNs.

Tumor cell entry into lymphatic vessels is essential for cancer metastasis.²² We subsequently determined whether LMW-HA promotes melanoma cell entry into lymphatic vessels by examining lymphatic morphological changes in the feet of mice by immunostaining with LYVE-1, a specific lymphatic endothelial cell marker. The results demonstrated that peritumoral lymphatic vessels were significantly enlarged in LMW-HA-treated mice, whereas HMW-HA had no effect (Figs. 1C and D). To further identify whether the intercellular adhesion of dilated lymphatic vessels was disrupted by LMW-HA, VE-cadherin, an endothelial cell-specific member of the cadherin family responsible for regulating endothelial cell connections, was detected by immunofluorescence. Podoplanin, another lymphatic vessel-specific marker, was simultaneously stained to locate the lymphatic lumen. Compared with HMW-HA- and medium-treated mice, LMW-HA-treated mice exhibited faint and indistinct VE-cadherin staining, as determined by confocal imaging, indicating that lymphatic endothelial intercellular adhesion was impaired by LMW-HA (Fig. 1E). These results suggest that LMW-HA promotes tumor lymphatic metastasis by opening lymphatic endothelial cell junctions. Then, we tested tumor weights and did not detect any differences among the three groups (Fig. 1F). These results exclude the possibility that LMW-HA contributes to lymphatic metastasis by promoting tumor cell growth.

LMW-HA increases interstitial-lymphatic flow in mice

Based on the results shown in Fig. 1, it is likely that LMW-HA accelerates melanoma cell migration from the interstitial space to the lymphatic vessel lumen by regulating lymphatic endothelial cell junctions *in vivo*. To test this hypothesis, an experiment on rapid transit of macromolecules from the interstitium to lymphatic vessels was performed to mimic tumor cell flow by using high-molecular-weight tissue-impermeable FITC-dextran (~2,000 kDa), a standard lymphatic imaging agent that can enter lymphatic vessels from the interstitial space after inoculation. As shown in Fig. 2, in contrast to medium treatment

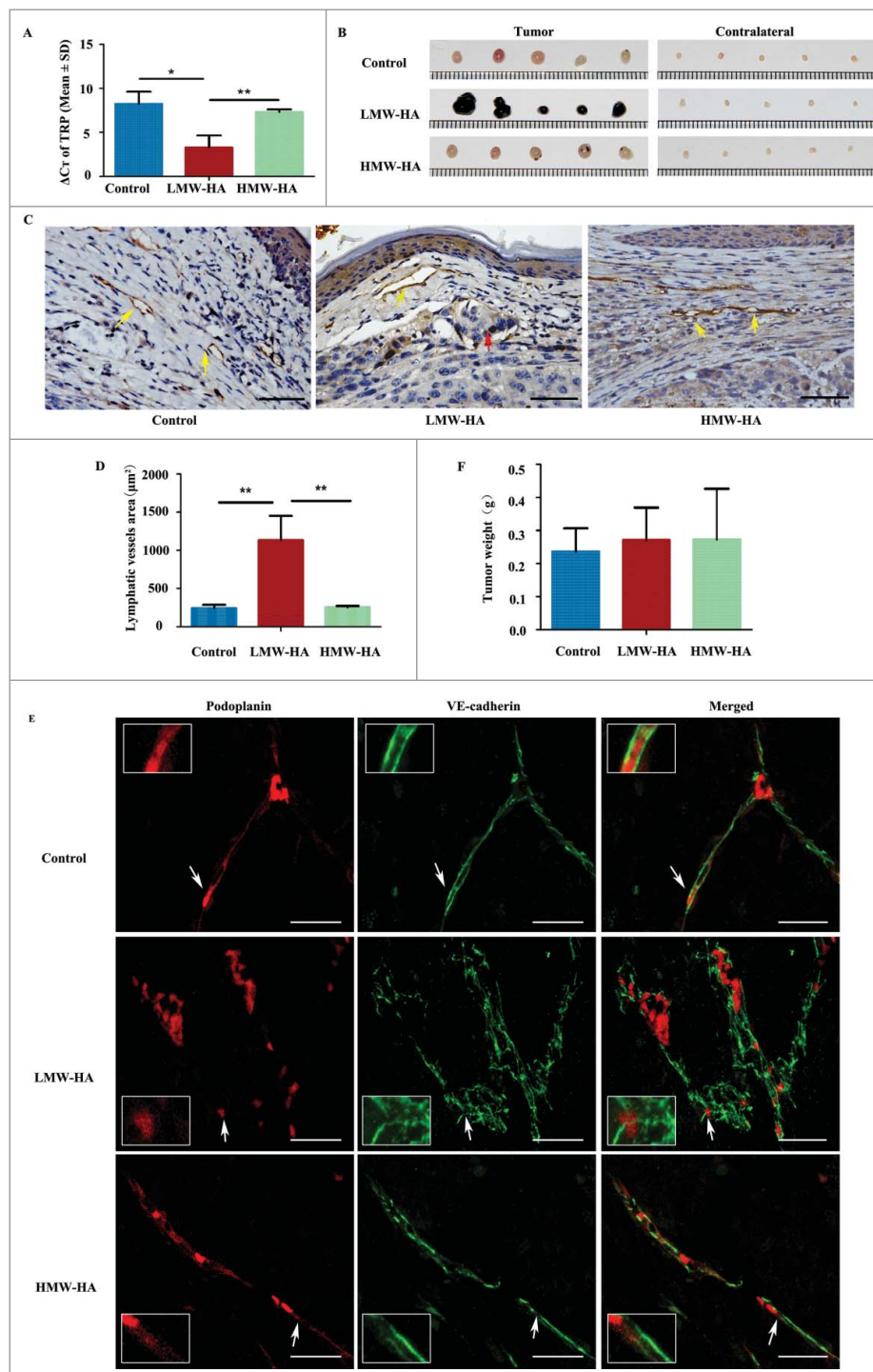


Figure 1. LMW-HA enhances B16F10 cell metastasis to lymph nodes *in vivo*. (A) Quantification of the mRNA levels of the melanoma marker TRP-1 in lymph nodes by qRT-PCR on day 7 after the first inoculation. TRP-1 mRNA levels in the lymph nodes of LMW-HA-, HMW-HA-, and medium-treated mice were calculated. $\Delta C_T = C_T$ (TRP) – C_T (GAPDH). Bars represent the mean \pm SD. Three experiments involving LMW-HA-, HMW-HA-, and medium-treated mice were performed, with five mice in each group, $n = 3$, $*p < 0.05$, $**p < 0.01$, ANOVA. (B) Representative photographs of the right popliteal LNs from mice 17 d after inoculation with B16F10 + LMW-HA, B16F10 + HMW-HA, and B16F10 + medium are shown on the left panels. Black metastatic foci were visible because the B16F10 cells produced melanin pigments. Contralateral LNs of mice are shown on the right panels. (Scale in mm) (C) Routine immunohistochemical assays of representative lymphatic vessels of the footpad sections of LMW-HA-, HMW-HA-, and medium-treated groups are shown using anti-LYVE-1 antibody. Yellow arrows emphasize LYVE-1-positive lymphatic vessels. Red arrows indicate melanoma cells in enlarged lymphatic vessels. (Scale bars: $50 \mu\text{m}$). (D) Sizes of lymphatic vessels were compared among LMW-HA-, HMW-HA-, and medium-treated mice, $n = 5$, $**p < 0.01$, ANOVA. (E) LMW-HA decreases lymphatic intercellular adhesion *in vivo*. Confocal imaging of footpad sections immunostained for podoplanin (red) and VE-cadherin (green). The results are shown in representative images of the findings from three experiments, with five animals per condition per experiment (indicated by the white arrows). (Scale bars: $25 \mu\text{m}$). (F) The tumor weights of these mice were measured, $n = 5$, ANOVA.

($99 \pm 8\%$), LMW-HA appeared to accelerate the clearance of FITC-dextran, as the fluorescence near the injection site was $65 \pm 21\%$ at 2 h after stimulation with LMW-HA, whereas

HMW-HA administration did not increase leakage ($105 \pm 9\%$). These results suggest that LMW-HA plays an important role in facilitating interstitial-lymphatic flow *in vivo*.

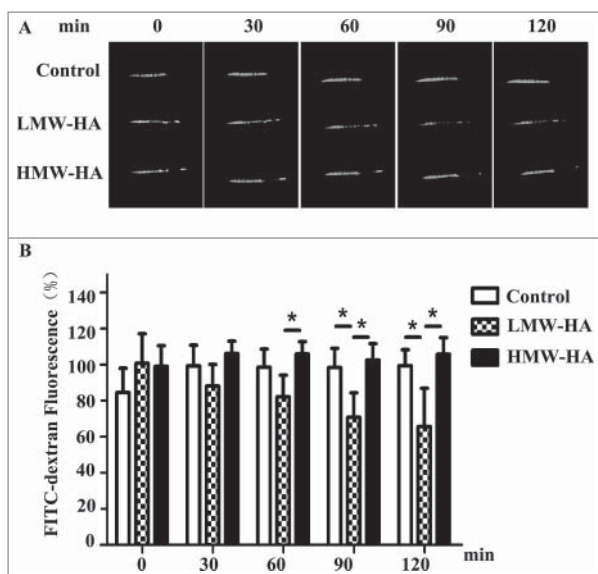


Figure 2. LMW-HA enhances interstitial-lymphatic flow in C57BL/6 mice. (A) A total of 20 μL of high-molecular-weight FITC-dextran (8 mg/mL) was intradermally co-injected with LMW-HA (5 μg), HMW-HA (5 μg), or medium (control) into the tails of mice (female, 8 weeks old). Five mice were used in each experimental group. Photographs were taken under LED illumination every 30 min until 120 min had elapsed. A representative sample of five mice is shown. FITC-dextran fluorescence near the injection site was measured. (B) Fluorescence intensities at the initial time (0 min) were set to 100%, and the fluorescence values at the other time points were calculated as the percentage of the value at 0 min. Bars represent the mean \pm SD, $n = 5$, * $p < 0.05$, ANOVA.

LMW-HA decreases lymphatic endothelial barrier function and increases permeability in HDLEC monolayers

Previous studies have reported that endothelial barrier function depends on intercellular junction integrity.²³ Therefore,

transendothelial electrical resistance (TEER) experiments were carried out to investigate the effects of LMW-HA on endothelial cell junction integrity *in vitro*. The results showed that maximal disruption of HDLEC monolayers was obtained by LMW-HA at 10 $\mu\text{g}/\text{mL}$. Substantially higher concentrations of LMW-HA (up to 20 $\mu\text{g}/\text{mL}$) did not further decrease TEER (Fig. S1). TEER remained steady for a prolonged period in HDLEC monolayers exposed to LMW-HA, confirming that a decrease in barrier function had occurred. Compared to baseline, there were no significant changes in TEER levels of monolayer exposed to HMW-HA (Fig. 3A). Then, we compared the relative impedance of quiescent HDLEC monolayers treated with positive control of VEGF-A, which caused an early increase in TEER levels, followed by a sustained decrease (Fig. 3A). The change in lymphatic endothelial cell monolayer permeability may also reflect the state of intercellular adhesion integrity. Therefore, to determine the effects of LMW-HA on HDLEC monolayer permeability, transwell assay was performed to measure the transfer of FITC-dextran (~ 40 kDa) from the upper chamber to the lower chamber. As shown in Fig. S2, stimulation with LMW-HA or VEGF-A significantly increased the migration of FITC-dextran across the cell monolayer compared to medium treatment (* $p < 0.05$). No significant differences were observed between the HMW-HA- and medium-treated groups. These results suggest that LMW-HA disrupts intercellular adhesion, resulting in enhanced permeability.

LMW-HA enhances migration of melanoma cells across HDLEC monolayers

After confirming that endothelial barrier disruption and permeability increasement were in the context of LMW-HA

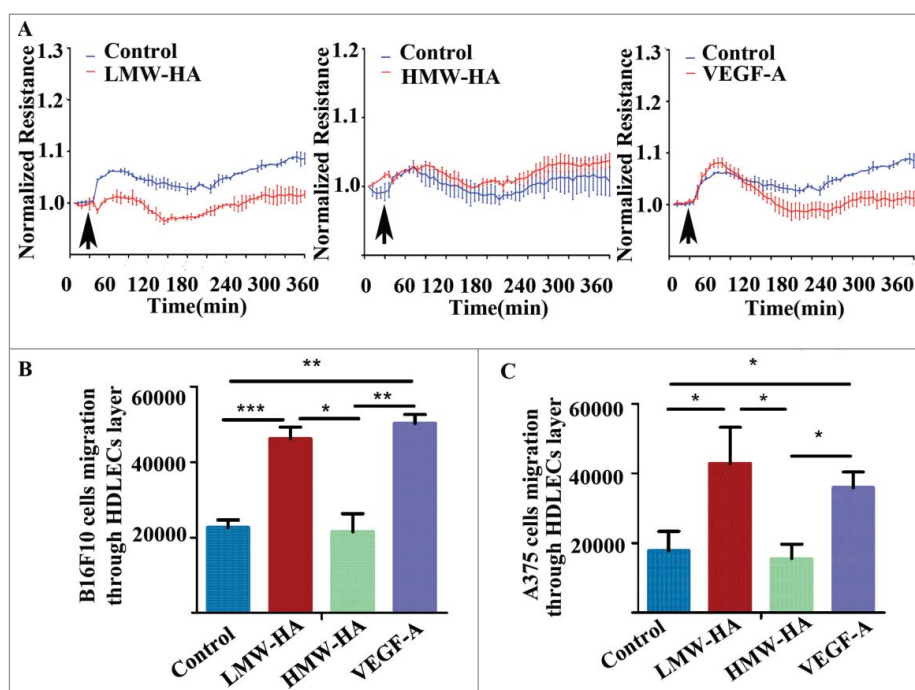


Figure 3. LMW-HA disrupts lymphatic endothelial cell barrier function and increases melanoma cell migration across the lymphatic endothelium. (A) Effects of LMW-HA (10 $\mu\text{g}/\text{mL}$), HMW-HA (10 $\mu\text{g}/\text{mL}$), VEGF-A (100 ng/mL), and medium on lymphatic endothelial barrier function were measured by transendothelial electrical resistance (TEER) in HDLECs ($n = 3$). The arrows indicate the times of addition. (B, C) Cumulative data regarding the numbers of B16F10 (B) and A375 (C) cells that migrated through the lymphatic endothelial cell monolayer were calculated, $n = 3$, * $p < 0.05$, ** $p < 0.01$, *** $p < 0.001$, ANOVA.

accumulation in the tumor microenvironment, we tested whether endothelial monolayer impairment accelerated melanoma cell migration across the lymphatic endothelium *in vitro*. As illustrated in Fig. 3B, B16F10 and A375 melanoma cells exhibited basal migration rates across the lymphatic endothelial monolayer without any stimulation. This migration was significantly higher when HDLECs were treated with LMW-HA or VEGF-A (Fig. 3B; Fig. S3A). To minimize the possible pro-migratory effects of LMW-HA on B16F10 and A375 cells, wound healing and transwell assays were carried out, and the results indicated that LMW-HA failed to affect B16F10 and A375 cell migration (Figs. S3B–E). These results indicate that the effects of LMW-HA on melanoma cell trans-lymphatic endothelial migration are due to lymphatic endothelial intercellular adhesion disruption, not promotion of melanoma cell migration.

LMW-HA induces disruption of lymphatic endothelial adhesion mediated by VE-cadherin in HDLEC monolayers

Based on the finding that LMW-HA disrupts the connections between lymphatic endothelial cells, we subsequently attempted to determine the underlying mechanism. VE-cadherin is a marker of endothelial adherens junctions that mediates homotypic cell–cell adhesion by associating with β -catenin and cortical actin cytoskeletal components to maintain integrity.²⁴ Interestingly, it has been demonstrated that VE-cadherin is required for maintenance of lymphatic integrity.²⁵ To test if LMW-HA opens lymphatic endothelial cell link by

compromising VE-cadherin-, β -catenin-, and F-actin-mediated intercellular adhesion, we analyzed the subcellular localization of these molecules in HDLEC monolayers using immunofluorescence confocal microscopy (Fig. 4A). Without stimulation, VE-cadherin and β -catenin distributed at the plasma membrane, whereas F-actin localized around the cell periphery. After treatment with LMW-HA or VEGF-A for 2 h, VE-cadherin diminished at the plasma membrane, and the junctions were discontinuous and exhibited small gaps. Additionally, β -catenin exhibited a disorganized arrangement. We also observed numerous stress fibers traversing the cell body. However, there were no obvious morphological changes after addition of HMW-HA. These data suggest that LMW-HA increases lymphatic endothelial permeability and disrupts barrier integrity by unscrewing intercellular junctions.

Given that phosphorylation of VE-cadherin- β -catenin results in endocytosis of VE-cadherin²⁶ and leads to disruption of intercellular adhesion, we next performed western blotting experiments to measure the levels of VE-cadherin- β -catenin phosphorylation and the changes in intracytoplasmic VE-cadherin content. The results showed that VE-cadherin phosphorylation at Tyr731, β -catenin phosphorylation at Tyr142, and VE-cadherin cytoplasmic localization were markedly increased following LMW-HA treatment (Fig. 4B; Fig. S4A and S6). Similar results were obtained from VEGF-stimulation, whereas no obvious changes were observed in the HMW-HA group. These results indicate that LMW-HA decreases VE-cadherin-mediated intercellular adhesion.

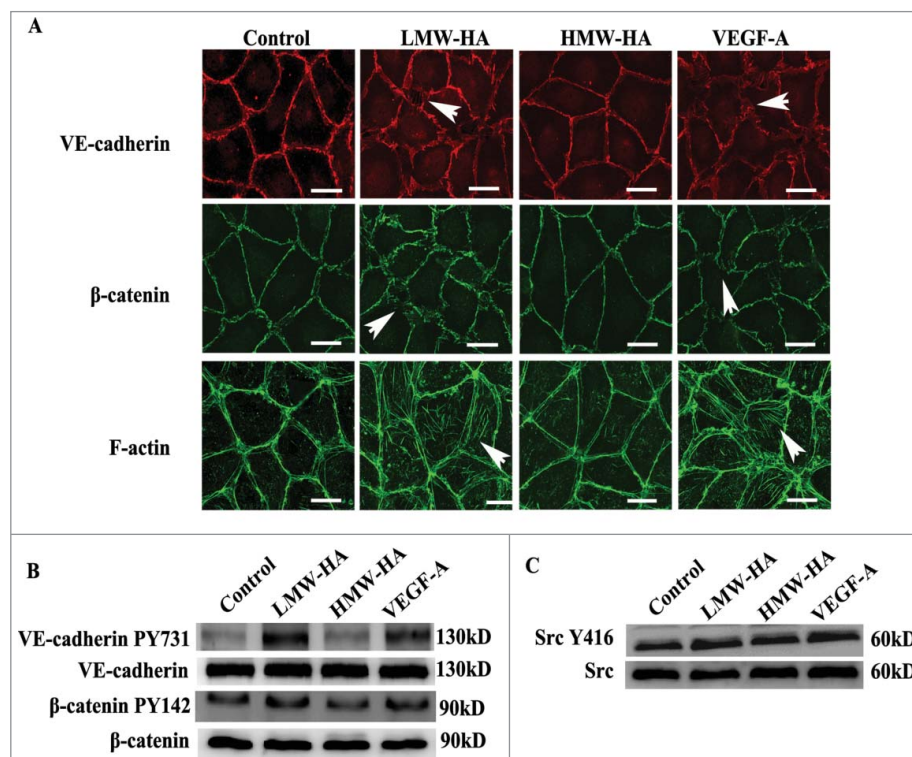


Figure 4. Mechanism studies of the effects of LMW-HA on lymphatic intercellular adhesion. (A) Effects of LMW-HA on VE-cadherin, β -catenin and F-actin localization in HDLECs were evaluated by immunofluorescence and phalloidin staining. After treatment with LMW-HA (10 μ g/mL) or VEGF-A (100 ng/mL) for 2 h, VE-cadherin (red) and β -catenin (green) became disorganized, and numerous stress fibers (green) traversing the cell body were observed (as indicated by the white arrows). Cells were visualized under a confocal microscope. One representative image of three experiments is shown. (Scale bars: 25 μ m.). (B, C) The levels of VE-cadherin, β -catenin, and Src phosphorylation in HDLECs were measured. HDLECs were stimulated with 10 μ g/mL of LMW-HA, 10 μ g/mL of HMW-HA, 100 ng/mL of VEGF-A, or medium for 30 min. Stimulated cell lysates were subjected to immunoblot analysis with the indicated antibodies. GAPDH was the loading control.

LMW-HA stimulates Src phosphorylation and increases intracellular calcium levels in HDLECs

Src-mediated phosphorylation of VE-cadherin at tyrosine Y731 has been linked to vascular permeability impairments mediated by some inflammatory regulators and growth factors.²⁷ However, LMW-HA, a main non-cellular pro-inflammatory molecule, has never been reported to promote VE-cadherin phosphorylation through Src activation. VE-cadherin mediated increase of cytosolic Ca²⁺ precedes changes in endothelial cell shape and the opening of inter-endothelial junctions.²⁸ To further determine the molecular mechanism underlying LMW-HA-induced disruption of lymphatic endothelial cell adhesion, Src phosphorylation, and Ca²⁺ signaling were evaluated. We found that the levels of phosphor-Src (Fig. 4C; Fig. S6) and intracellular Ca²⁺ were increased in LMW-HA- and VEGF-A-stimulated HDLECs (Fig. S4B). No significant differences were found between the HMW-HA and medium groups. These results

demonstrate that Src and Ca²⁺ signal pathways participate in LMW-HA-mediated lymphatic endothelial integrity disruption.

Antibodies against LYVE-1 inhibits LMW-HA-enhanced or -stimulated effects on HDLECs

To further identify if LMW-HA is responsible for the impairment of HDLEC intercellular junctions, the main LMW-HA receptor in lymphatic endothelial cells (LYVE-1) was priorly blocked before all experiments. Isotype IgG was used as a control. The results showed that all experiments in LMW-HA-treated groups were returned toward their original states (Fig. 5, Figs. S5 and S6). Isotype control IgG did not exhibit any restorative effects in corresponding experiments. These results demonstrate that LMW-HA has the ability to disrupt lymphatic endothelial cell-cell contacts.

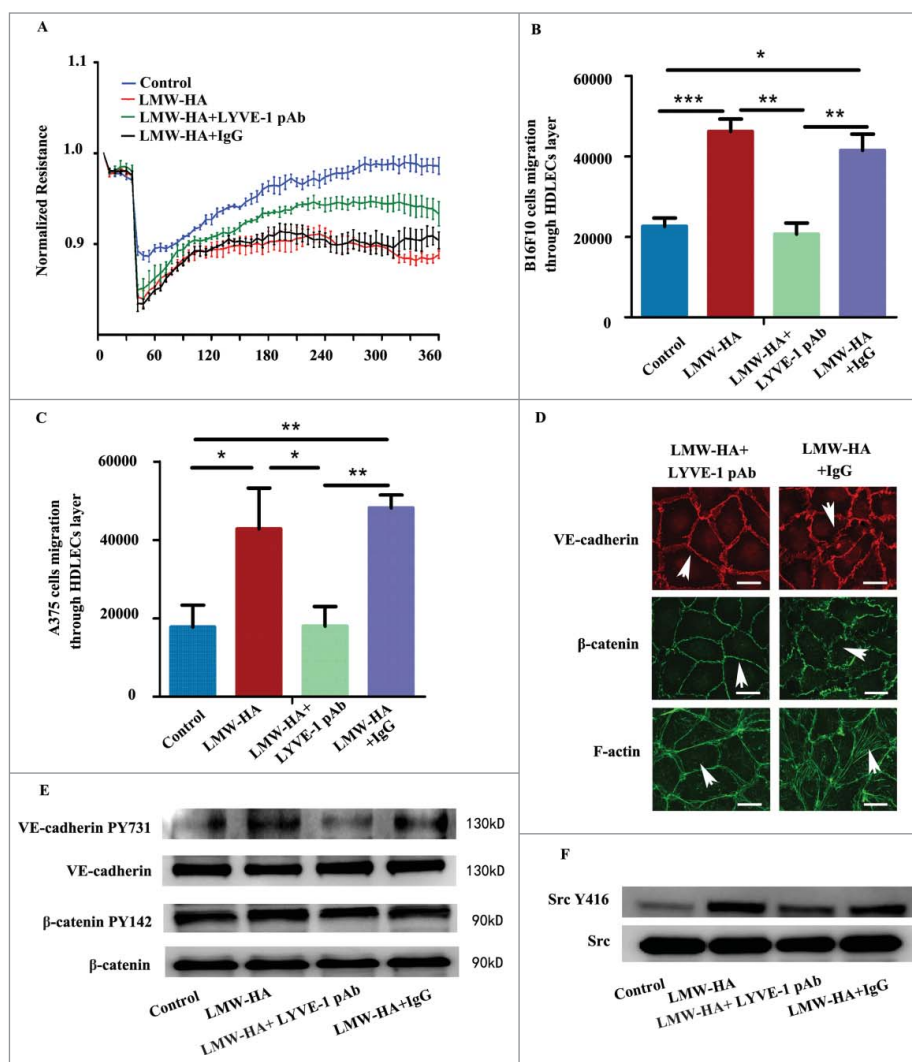


Figure 5. Antibodies against lymphatic vessel endothelial hyaluronan receptor-1 inhibit the effects of LMW-HA on HDLECs. All HDLECs were pre-incubated with 10 μ g/mL LYVE-1 neutralizing antibody or isotype IgG. (A) TEER assays were performed to measure lymphatic endothelial barrier function. (B, C) Effects of LMW-HA on melanoma cell migration through the lymphatic endothelial cell monolayer were detected, $n = 3$, * $p < 0.05$, ** $p < 0.01$, *** $p < 0.001$, ANOVA. (D) The distributions of VE-cadherin, β -catenin, and F-actin were evaluated by immunocytofluorescent assays, and the morphologies of VE-cadherin, β -catenin, and F-actin returned to their original states (as indicated by the white arrows). (E) VE-cadherin phosphorylation and β -catenin phosphorylation were detected by western blotting, $n = 3$, * $p < 0.05$, ANOVA. (F) Src phosphorylation was detected by western blotting, $n = 3$, * $p < 0.05$, ANOVA.

Discussion

The aim of this study was to investigate whether LMW-HA modulates tumor cell metastasis to LNs. Early metastasis to LNs is a frequent complication in human melanoma.²⁹ Here, we used melanoma as the model to study the role of LMW-HA on accelerating LN metastasis. We found that LMW-HA enhanced B16F10 melanoma cell migration from the footpad to the popliteal LNs of mice (Fig. 1), a finding consistent with the notion that LMW-HA is associated with lymphatic vessel invasion by tumor cells.^{10,11} We also found increases in tumor-draining lymphatic vessel diameter in LMW-HA-treated mice. This result is consistent with that of a recent study demonstrating that changes in the adhesive properties of the lymphatic endothelium near tumors are fundamental steps in tumor metastasis through the lymph vessel lumen.^{18,30} We next evaluated whether LMW-HA could regulate intercellular adhesion of dilated lymphatic vessels by examining VE-cadherin expression patterns. The results showed that the distribution of VE-cadherin was dramatically altered in mouse footpads of LMW-HA-treated group compared with HMW-HA-treated and control mice, suggesting that decreased VE-cadherin-mediated intercellular adhesion may be associated with tumor lymphatic metastasis accelerated by LMW-HA. Similarly, a previous report showed that LMW-HA disrupted the blood vessel barrier and resulted in circulating metastasis of carcinoma cells.³¹ Based on these findings, we presumed that melanoma cells in the interstitial space migrated into the lymphatic vessel lumen with the assistance of LMW-HA, which expands lymphatic vessels and leads to an increased fluid drainage. This hypothesis was supported by the results obtained by Huang and her colleagues, who stated that the ligands (including HA and a group of growth factors/cytokines-containing CRS motifs) of CRSBP-1 (also termed LYVE-1) induce opening of lymphatic intercellular junctions, allowing rapid transit of macromolecules and/or cells from the interstitium into lymphatic vessels in wide-type but not CRSBP-1/LYVE-1-null animals.³² In addition, we observed that HA oligosaccharides significantly lowered macromolecule fluorescence in mice tails (Fig. 2), while HA polymers did not, suggesting that LMW-HA facilitates tumor cell invasion into lymphatic vessels by increasing interstitial-lymphatic flow. Our findings suggest that elevated lymphatic dissemination of melanoma results from abnormal accumulation of hyaluronan oligosaccharides, which break endothelial cell junctions and facilitate melanoma cell migration into lymphatic vessels.

To confirm our results, we subsequently investigated whether LMW-HA impairs endothelial continuity at the cellular level. Vascular permeability is one of the important factors that make the vascular endothelium susceptible to tumor invasion into vascular systems.³³ Studies have implied that LMW-HA affects the integrity of adherens junctions and promotes increased vascular permeability *in vitro*.³¹ Our study demonstrated that LMW-HA, in addition to disrupting vascular barriers, could also break the lymphatic endothelial integrity (Fig. 3A; Fig. S2). Previous studies have shown that downregulation of the lymphatic endothelial monolayer can induce fibrosarcoma migration through the lymphatic endothelial monolayer *in vitro* and facilitate sarcoma cells entering the lymphatic circulation.¹⁸ Consistent with these findings, we observed that endothelial monolayers activated by LMW-HA were easier for melanoma cells to pass into the lower chamber

(Fig. 3B; Fig. S3A), which may indicate that a relationship exists between lymphatic barrier disruption by LMW-HA and LN metastasis in melanoma. This model reliably reproduced our *in vivo* finding that LMW-HA-accelerated melanoma cell breaking into lymphatic vessels.

The mechanisms underlying the effects of LMW-HA on lymphatic lumen integrity are poorly defined. Some reports have shown that PDGF-BB or VEGF-A disrupts lymphatic intercellular adhesion by inducing tyrosine phosphorylation and VE-cadherin internalization.³⁴ Our data demonstrated that LMW-HA-induced disorders of adhering molecules in lymphatic endothelial cells, such as disorganization of VE-cadherin and β -catenin at membrane junctions, formation of F-actin stress fiber traversing across the cell body (Fig. 4A), enhancement of VE-cadherin/ β -catenin phosphorylation (Fig. 4B; Fig. S6), and acceleration of VE-cadherin endocytosis (Fig. S4A). Additionally, Src Y416 and Ca^{2+} signaling assays indicated that conventional signaling pathway activation was available to interpret the destabilization of the cell-cell junction mediated by LMW-HA in lymphatic vessels. Further, we showed that blocking LYVE-1, the major receptor for LMW-HA, attenuated the disruption of lymphatic endothelial cell adhesion (Fig. 5; Figs. S5 and S6), indicating that LMW-HA regulates the distinct patterns of endothelial cell connections through specific receptors. All these data indicated that LMW-HA might serve as a non-cytokine activator in modulating lymph vessel endothelial cell junctions.

Conclusions

In summary, the novel function of LMW-HA in tumor lymphatic metastasis was well characterized in this study, as we determined that LMW-HA promotes tumor lymphatic metastasis by disrupting lymphatic endothelial cell junctions. This finding has provided us with new insight into the role of LMW-HA in tumor metastasis and may be helpful to therapeutic interventions in targeting LMW-HA generation or specific inhibition of LMW-HA-related signaling pathways in the future.

Materials and methods

Reagents

High-molecular-weight hyaluronan (HA15M-5, Mw: 1.01×10^3 kDa– 1.8×10^3 kDa, Mw/Mn: $1.131 \pm 1.002\%$) and hyaluronan oligosaccharides (HA5K-5, Mw: <10 kDa) were obtained from Lifecore.

Cell culture

B16F10 mouse melanoma and A375 human melanoma cells were obtained from American Type Culture Collection, where they were authenticated using short tandem repeat analysis and passaged for a maximum of 2 mo post-resuscitation. Cells were grown in DMEM supplemented with 10% (vol/vol) fetal bovine serum (FBS, Gibco). Human dermal lymphatic endothelial cells (HDLECs) were obtained from PromoCell (C-12216) in January 2015. They were certified by PromoCell in September 2013

and tested for cell morphology and cell-type specific markers using immunofluorescent staining. Cell viability and cell population doubling (PD) time in log phase were also tested by the ISO13319 and PDL tests. Microbiological contaminants and infectious viruses were examined by direct plating and PCR. All cells were maintained in endothelial cell MV2 growth medium (PromoCell, C-22121), and all experiments were performed between passages 3 and 8.

Mice

Seven-week-old female C57BL/6 mice were obtained from Shanghai SLAC Laboratory Animal Co., Ltd. All experimental protocols were approved by the appropriate institutional review board.

In vivo metastasis studies

Mice were subjected to tumor lymphatic metastasis as previously described.²⁹ B16F10 cells (2×10^6) in 50 μ L of PBS were injected into the right hind footpad on day 0. Mice pre-injected with tumor cells were separately injected in the footpad region with 5 μ g of LMW-HA, 5 μ g of HMW-HA, or nothing in 25 μ L of PBS, daily for the next 5 d, followed by three times per week until they were sacrificed on day 17.

Quantitative real-time polymerase chain reaction analyses

On day 7, the right popliteal LNs were dissected and pooled for each group of five mice to quantify tumor burden by qRT-PCR as described.³⁵ Total RNA was isolated from the LNs, and the mRNA expression levels of different target genes were determined using standard procedures. Threshold cycle (C_T) values were assigned to various products according to the cycle number. $\Delta C_T = C_T$ (tyrosinase-related protein (TRP)) - C_T (glyceraldehyde-3-phosphate dehydrogenase (GAPDH)). The following primers were used: TRP, F: 5'-GAAAATATGACCCTGCTGTTCGA-3' and R: 5'-TTGTCTCCCGTTCCATTCA-3'; GAPDH, F: 5'-CGTGTCC-TACCCCAATGT-3' and R: 5'-TGTCATCATACTTGGCAGG-TTTCT-3' (where F = forward, and R = reverse).

Immunohistochemistry and Immunofluorescence

On day 17, the mice were killed, and their footpads were collected and fixed overnight in 10% (v/v) phosphate-buffered formalin. Tissues fixed in formalin were embedded in paraffin, and then 5 μ m cryostat sections were cut. Immunohistochemistry analyses were performed as described,³⁶ using antibodies against LYVE-1 (ab14917, Abcam). The sections were stained by immunofluorescence as described,³⁷ and anti-mouse podoplanin (ab11936, Abcam), anti-mouse VE-cadherin (sc-6458, Santa Cruz), Alexa647- or Alexa488-coupled secondary antibodies were used to detect reactive products.

Computer-assisted morphometric analyses

Immunohistochemistry stains of the footpad sections for LYVE-1 were analyzed using Image Pro-Plus 6.0 software as previously described.³⁸ Average lymphatic vessel size was determined in the footpad area.

Fluorescein isothiocyanate-dextran tail injection assay

FITC-dextran tail injection assays were carried out as described.³⁴ To evaluate interstitial-lymphatic transit in mice (five female mice per experimental group), 20 μ L of 8 mg/mL fluorescein isothiocyanate (FITC)-dextran (MW \sim 2,000 kDa, Sigma) with LMW-HA (5 μ g/20 μ L), HMW-HA (5 μ g/20 μ L) or medium were separately injected intradermally into the tails of C57BL/6 mice. Progressive diffusion (in the absence of injection pressure) of fluorescence near the injection site was monitored with the Bio-Rad ChemiDocTM Imaging System (Tina Cuccia). Fluorescence intensities were determined using the NIH Image J program following photography. Fluorescence values at other time points were calculated as the percentage of the value at 0 min. The interstitial-lymphatic transit analysis appeared to be quantitative and specific as previously reported.³²

Measurement of transendothelial electrical resistance

TEER across the endothelial cell monolayer was measured using an impedance sensor system (Applied Biophysics). Confluent HDLECs were monitored for 30 min to establish baseline resistance. Then, the HDLECs were exposed to LMW-HA (5–20 μ g/mL), HMW-HA (10 μ g/mL), VEGF-A (100 ng/mL, ab194172, Abcam), or medium. In this study, VEGF-A was used as a positive control, because 100 ng/mL of VEGF-A has been shown to disrupt lymphatic endothelial integrity by regulating the VE-cadherin pathway.^{13,34} Values from each microelectrode were pooled at discrete time points and plotted versus time as the mean \pm SE of the mean.

Tumor transendothelial migration assay

Transendothelial migration assays were performed using the CytoSelectTM Tumor Transendothelial Migration Assay kit (Cell Biolabs CBA-216), according to the manufacturer's instructions. Briefly, monolayers of HDLECs on porous inserts (8 μ m) in 24-well plates were separately treated with LMW-HA, HMW-HA, VEGF-A, and medium for 12 h to regulate the junctions between endothelial cells. B16F10 and A375 melanoma cells were labeled with CytotrackerTM (green fluorescence), mixed with equal volumes of LMW-HA, HMW-HA, VEGF-A, or medium and placed over the endothelial monolayer. After 20 h, non-migratory cells were removed, and cells migrating across the endothelial monolayer were scanned under confocal microscopy (Nikon A1). At least five microscopic fields of view were observed for each condition. Next, the inserts were transferred into wells containing lysis buffer. Readings were measured using a monochromator-based multi-mode microplate reader (480 nm/520 nm, Synergy 4) with 100 μ L of aliquots.

Immunofluorescence assay

The distributions of VE-cadherin, β -catenin, and F-actin were analyzed by immunofluorescence assays. 100% confluent HDLECs were treated with LMW-HA, HMW-HA, VEGF-A, or medium for 2 h and then stained to detect the distributions of VE-cadherin and β -catenin by immunofluorescence as

described.³⁹ Anti-VE-cadherin antibody (ab7047, Abcam) and anti- β -catenin antibody (ab32572, Abcam) were used to detect reactive products. To demonstrate changes of actin filaments, cells were labeled with FITC-phalloidin (Cytoskeleton). Coverslips were then placed on the slides using glycerol as a mountant and visualized under confocal microscopy (Nikon A1).

Phosphorylation measurements

HDLECs were harvested after treatment with LMW-HA, HMW-HA, VEGF-A, or medium for 30 min. Protein expression was determined by western blotting using standard techniques. VE-cadherin mAb (ab7047, Abcam), phosphor-VE-cadherin pAb (ab27776, Abcam), β -catenin mAb (ab32572, Abcam), phosphor- β -catenin pAb (ab27798, Abcam), Src mAb (32G6, CST), phosphor-Src mAb (D49G4, CST), and GAPDH mAb (ab9484, Abcam) were used separately. Images were analyzed using Image Pro-Plus 6.0 software.

LMW-HA-LYVE-1 interaction assay

To determine if LMW-HA was responsible for the impairment of HDLEC intercellular junction, HDLECs were pre-treated with neutralizing anti-LYVE-1 antibodies (AF2089, R&D). Then, the cells were treated with LMW-HA as described above. Isotype-matched non-immune IgG (AB-108-C, R&D) was added to parallel cultures as a control.

Statistical analysis

Analysis of variance (ANOVA) was used to compare differences among groups ($n \geq 3$). Student's *t* test was used for comparisons between two different groups. Analyses were performed using SPSS 13.0 statistical software. A *p* value <0.05 was considered statistically significant. At least three independent experiments were performed for each assay.

Disclosure of potential conflicts of interest

No potential conflicts of interest were disclosed.

Funding

This work was supported by the National Natural Science Foundation of China (81172027, 81502490, 81402419, 81502491, 81572821, and 81272479), the Sailing Program of Shanghai Committee of Science and Technology (14YF1412200), the Program of Shanghai Leading Talents (2013-038), the Program of Shanghai Shen-Kang Hospital Development Center (SHDC22014004), and the Yuyan Program of Shanghai Jiao Tong University Affiliated Sixth People's Hospital (LY34.Zongyu-0112).

Ethics approval and consent to participate

All experimental protocols were approved by the Institutional Review Board.

Author contributions

Feng Gao, Yan Du, and Manlin Cao designed the research; Yan Du, Yiwen Liu, Yiqing He, Cuixia Yang, and Man Wu performed the research; Yan

Du, Manlin Cao, Yiqing He, and Guoliang Zhang analyzed the data; and Feng Gao, Yan Du, Cuixia Yang, and Guoliang Zhang wrote the paper.

References

1. Tarhini AA, Zahoor H, Yearley JH, Gibson C, Rahman Z, Dubner R, Rao UN, Sander C, Kirkwood JM. Tumor associated PD-L1 expression pattern in microscopically tumor positive sentinel lymph nodes in patients with melanoma. *J Transl Med* 2015; 13:319; PMID:26419843; <http://dx.doi.org/10.1186/s12967-015-0678-7>
2. Pein M, Oskarsson T. Microenvironment in metastasis: roadblocks and supportive niches. A Review in the Theme: Cell and Molecular Processes in Cancer Metastasis. *Am J Physiol Cell Physiol* 2015;ajpcell 00145 2015; 309(10):C627-38; PMID:26377313; <http://dx.doi.org/doi:10.1152/ajpcell.00145.2015>
3. Cox TR, Erler JT. Remodeling and homeostasis of the extracellular matrix: implications for fibrotic diseases and cancer. *Dis Model Mech* 2011; 4:165-78; PMID:21324931; <http://dx.doi.org/10.1242/dmm.004077>
4. Oskarsson T. Extracellular matrix components in breast cancer progression and metastasis. *Breast* 2013; 22 (Suppl 2):S66-72; PMID:24074795; <http://dx.doi.org/10.1016/j.breast.2013.07.012>
5. Jiang D, Liang J, Noble PW. Hyaluronan in tissue injury and repair. *Annu Rev Cell Dev Biol* 2007; 23:435-61; PMID:17506690; <http://dx.doi.org/10.1146/annurev.cellbio.23.090506.123337>
6. Yang C, Cao M, Liu H, He Y, Xu J, Du Y, Liu Y, Wang W, Cui L, Hu J et al. The high and low molecular weight forms of hyaluronan have distinct effects on CD44 clustering. *J Biol Chem* 287:43094-107; PMID:23118219; <http://dx.doi.org/10.1074/jbc.M112.349209>
7. Wolny PM, Banerji S, Gounou C, Brisson AR, Day AJ, Jackson DG, Richter RP. Analysis of CD44-hyaluronan interactions in an artificial membrane system: insights into the distinct binding properties of high and low molecular weight hyaluronan. *J Biol Chem* 285:30170-80; PMID:20663884; <http://dx.doi.org/10.1074/jbc.M110.137562>
8. Lokeshwar VB, Obek C, Soloway MS, Block NL. Tumor-associated hyaluronic acid: a new sensitive and specific urine marker for bladder cancer. *Cancer Res* 1997; 57:773-7; PMID:9044859
9. Franzmann EJ, Schroeder GL, Goodwin WJ, Weed DT, Fisher P, Lokeshwar VB. Expression of tumor markers hyaluronic acid and hyaluronidase (HYAL1) in head and neck tumors. *Int J Cancer* 2003; 106:438-45; PMID:12845686; <http://dx.doi.org/10.1002/ijc.11252>
10. Schmaus A, Klusmeier S, Rothley M, Dimmler A, Sipos B, Faller G, Thiele W, Allgayer H, Hohenberger P, Post S et al. Accumulation of small hyaluronan oligosaccharides in tumour interstitial fluid correlates with lymphatic invasion and lymph node metastasis. *British J Cancer* 2014; 111(3):559-67; PMID:24937668; <http://dx.doi.org/10.1038/bjc.2014.332>
11. Wu M, Cao M, He Y, Liu Y, Yang C, Du Y, Wang W, Gao F. A novel role of low molecular weight hyaluronan in breast cancer metastasis. *FASEB J* 2015; 29:1290-8; PMID:25550464; <http://dx.doi.org/10.1096/fj.14-259978>
12. Yu M, Zhang H, Liu Y, He Y, Yang C, Du Y, Wu M, Zhang G, Gao F. The cooperative role of S1P3 with LYVE-1 in LMW-HA-induced lymphangiogenesis. *Exp Cell Res* 2015; 336:150-7; PMID:26116468; <http://dx.doi.org/10.1016/j.yexcr.2015.06.014>
13. Karaman S, Detmar M. Mechanisms of lymphatic metastasis. *J Clin Invest* 2014; 124:922-8; PMID:24590277; <http://dx.doi.org/10.1172/JCI71606>
14. Podgrabsinska S, Skobe M. Role of lymphatic vasculature in regional and distant metastases. *Micro Res* 2014; 95:46-52; PMID:25026412; <http://dx.doi.org/10.1016/j.mvr.2014.07.004>
15. Jiang M, Qin C, Han M. Primary breast cancer induces pulmonary vascular hyperpermeability and promotes metastasis via the VEGF-PKC pathway. *Mol Carcinog* 2015; 55(6):1087-95; PMID:26152457; <http://dx.doi.org/10.1002/mc.22352>
16. Zheng W, Nurmi H, Appak S, Sabine A, Bovay E, Korhonen EA, Orsenigo F, Lohela M, D'Amico G, Holopainen T et al. Angiopoietin 2 regulates the transformation and integrity of lymphatic endothelial cell junctions. *Genes Dev* 2014; 28:1592-603; PMID:25030698; <http://dx.doi.org/10.1101/gad.237677.114>

17. Du LC, Chen XC, Wang D, Wen YJ, Wang CT, Wang XM, Kan B, Wei YQ, Zhao X. VEGF-D-induced draining lymphatic enlargement and tumor lymphangiogenesis promote lymph node metastasis in a xenograft model of ovarian carcinoma. *Reprod Biol Endocrinol* 2014; 12:14; PMID:24502459; <http://dx.doi.org/10.1186/1477-7827-12-14>
18. Yanagawa T, Shinozaki T, Watanabe H, Saito K, Raz A, Takagishi K. Vascular endothelial growth factor-D is a key molecule that enhances lymphatic metastasis of soft tissue sarcomas. *Exp Cell Res* 2012; 318:800-8; PMID:22326461; <http://dx.doi.org/10.1016/j.yexcr.2012.01.024>
19. Lennon FE, Mirzapioazova T, Mambetsariev N, Mambetsariev B, Salgia R, Singleton PA. Transactivation of the receptor-tyrosine kinase ephrin receptor A2 is required for the low molecular weight hyaluronan-mediated angiogenesis that is implicated in tumor progression. *J Biol Chem* 2014; 289:24043-58; PMID:25023279; <http://dx.doi.org/10.1074/jbc.M114.554766>
20. Singleton PA. Hyaluronan regulation of endothelial barrier function in cancer. *Adv Cancer Res* 2014; 123:191-209; PMID:25081530; <http://dx.doi.org/10.1016/B978-0-12-800092-2.00007-1>
21. Lennon FE, Singleton PA. Hyaluronan regulation of vascular integrity. *Am J Cardiovasc Dis* 2011; 1:200-13; PMID:22254199
22. van Zijl F, Krupitza G, Mikulits W. Initial steps of metastasis: cell invasion and endothelial transmigration. *Mutat Res* 2011; 728:23-34; PMID:21605699; <http://dx.doi.org/10.1016/j.mrrev.2011.05.002>
23. Komarova Y, Malik AB. Regulation of endothelial permeability via paracellular and transcellular transport pathways. *Annu Rev Physiol* 2010; 72:463-93; PMID:20148685; <http://dx.doi.org/10.1146/annurev-physiol-021909-135833>
24. Boccellino M, Camussi G, Giovane A, Ferro L, Calderaro V, Balestrieri C, Quagliuolo L. Platelet-activating factor regulates cadherin-catenin adhesion system expression and beta-catenin phosphorylation during Kaposi's sarcoma cell motility. *Am J Pathol* 2005; 166:1515-22; PMID:15855650; [http://dx.doi.org/10.1016/S0002-9440\(10\)62367-X](http://dx.doi.org/10.1016/S0002-9440(10)62367-X)
25. Kakei Y, Akashi M, Shigeta T, Hasegawa T, Komori T. Alteration of cell-cell junctions in cultured human lymphatic endothelial cells with inflammatory cytokine stimulation. *Lymphatic Res Biol* 2014; 12:136-43; PMID:25166264; <http://dx.doi.org/10.1089/lrb.2013.0035>
26. Orsenigo F, Giampietro C, Ferrari A, Corada M, Galaup A, Sigismund S, Ristagno G, Maddaluno L, Koh GY, Franco D et al. Phosphorylation of VE-cadherin is modulated by haemodynamic forces and contributes to the regulation of vascular permeability in vivo. *Nat Commun* 3:1208; PMID:23169049; <http://dx.doi.org/10.1038/ncomms2199>
27. Potter MD, Barbero S, Cheresin DA. Tyrosine phosphorylation of VE-cadherin prevents binding of p120- and beta-catenin and maintains the cellular mesenchymal state. *J Biol Chem* 2005; 280:31906-12; PMID:16027153; <http://dx.doi.org/10.1074/jbc.M505568200>
28. Sukriti S, Tauseef M, Yazbeck P, Mehta D. Mechanisms regulating endothelial permeability. *Pulmonary Circulat* 2014; 4:535-51; PMID:25610592; <http://dx.doi.org/10.1086/677356>
29. Kawada K, Sonoshita M, Sakashita H, Takabayashi A, Yamaoka Y, Manabe T, Inaba K, Minato N, Oshima M, Taketo MM. Pivotal role of CXCR3 in melanoma cell metastasis to lymph nodes. *Cancer Res* 2004; 64:4010-7; PMID:15173015; <http://dx.doi.org/10.1158/0008-5472.CAN-03-1757>
30. Chen XL, Nam JO, Jean C, Lawson C, Walsh CT, Goka E, Lim ST, Tomar A, Tancioni I, Uryu S et al. VEGF-induced vascular permeability is mediated by FAK. *Dev Cell* 2012; 22:146-57; PMID:22264731; <http://dx.doi.org/10.1016/j.devcel.2011.11.002>
31. Singleton PA, Dudek SM, Ma SF, Garcia JG. Transactivation of sphingosine 1-phosphate receptors is essential for vascular barrier regulation. Novel role for hyaluronan and CD44 receptor family. *J Biol Chem* 2006; 281:34381-93; PMID:16963454; <http://dx.doi.org/10.1074/jbc.M603680200>
32. Huang SS, Liu IH, Smith T, Shah MR, Johnson FE, Huang JS. CRSP-1/LYVE-1-null mice exhibit identifiable morphological and functional alterations of lymphatic capillary vessels. *FEBS letters* 2006; 580:6259-68; PMID:17070806; <http://dx.doi.org/10.1016/j.febslet.2006.10.028>
33. Sahni A, Arevalo MT, Sahni SK, Simpson-Haidaris PJ. The VE-cadherin binding domain of fibrinogen induces endothelial barrier permeability and enhances transendothelial migration of malignant breast epithelial cells. *Int J Cancer* 2009; 125:577-84; PMID:19358279; <http://dx.doi.org/10.1002/ijc.24340>
34. Hou WH, Liu IH, Tsai CC, Johnson FE, Huang SS, Huang JS. CRSP-1/LYVE-1 ligands disrupt lymphatic intercellular adhesion by inducing tyrosine phosphorylation and internalization of VE-cadherin. *J Cell Sci* 2011; 124:1231-44; PMID:21444752; <http://dx.doi.org/10.1242/jcs.078154>
35. Wiley HE, Gonzalez EB, Maki W, Wu MT, Hwang ST. Expression of CC chemokine receptor-7 and regional lymph node metastasis of B16 murine melanoma. *J Nat Cancer Institute* 2001; 93:1638-43; PMID:11698568; <http://dx.doi.org/10.1093/jnci/93.21.1638>
36. Schonthaler HB, Huggenberger R, Wculek SK, Detmar M, Wagner EF. Systemic anti-VEGF treatment strongly reduces skin inflammation in a mouse model of psoriasis. *Proc Natl Acad Sci U S A* 2009; 106:21264-9; PMID:19995970; <http://dx.doi.org/10.1073/pnas.0907550106>
37. Kajiya K, Hirakawa S, Detmar M. Vascular endothelial growth factor-A mediates ultraviolet B-induced impairment of lymphatic vessel function. *Am J Pathol* 2006; 169:1496-503; PMID:17003502; <http://dx.doi.org/10.2353/ajpath.2006.060197>
38. Paquet-Fifield S, Levy SM, Sato T, Shayan R, Karnezis T, Davydova N, Nowell CJ, Roufail S, Ma GZ, Zhang YF et al. Vascular endothelial growth factor-d modulates caliber and function of initial lymphatics in the dermis. *J Invest Dermatol* 2013; 133:2074-84; PMID:23439394; <http://dx.doi.org/10.1038/jid.2013.83>
39. Du Y, Liu Y, Wang Y, He Y, Yang C, Gao F. LYVE-1 enhances the adhesion of HS-578T cells to COS-7 cells via hyaluronan. *Clin Invest Med* 34:E45-54; PMID:21291635